Macromolecules

ARTICLE

pubs.acs.org/Macromolecules

Correlations between the Characteristic Rheological Quantities and Molecular Structure of Long-Chain Branched Metallocene Catalyzed Polyethylenes

Florian J. Stadler*,†,‡ and Vahid Karimkhani§

†Institute of Polymer Materials, Friedrich-Alexander University Erlangen-Nürnberg, Martensstrasse 7, D-91058 Erlangen, Germany

‡School of Semiconductor and Chemical Engineering, Chonbuk National University, Baekjero 567, Deokjin-gu, Jeonju, Jeonbuk, 561-756, Republic of Korea

§Department of Polymer Engineering, Amirkabir University of Technology, 424 Hafez Avenue, P.O. Box 15875-4413, Tehran, Iran

ABSTRACT: Different rheological quantities, such as the zero shear-rate viscosity η_0 and the linear steady-state elastic compliance J_e^0 of long-chain branched metallocene-catalyzed ethene homopolymers and ethene-/α-olefin copolymers with a polydispersity $M_w/M_n \approx 2$, were correlated with the molar mass M_w and degree of long-chain branching λ. A linear reference for the $\delta(|G^*|)$ plot was used to show the effect of long-chain branches on this rheological property. The linear steady-state elastic compliance J_e^0 correlated with the zero shear-rate viscosity increase factor η_0/η_0^{lin} and the characteristic phase angle δ_c. However, the latter only works when compensating for the influence of the molar mass on J_e^0 by the relationship between J_e^0 and M_w established elsewhere (Stadler and Münstedt, JoR, 2008). The characteristic phase angle δ_c and zero shear-rate viscosity enhancement factor η_0/η_0^{lin} are linked to each other by the linear dependencies for the type I and type II viscosity functions.

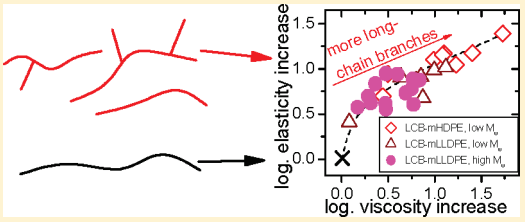

INTRODUCTION

The synthesis and characterization of long-chain branched metallocene catalyzed polyethylenes, both linear and short-chain branched, has attracted considerable interest.[1−5] This is due to major advantages of these products compared to those synthesized by Ziegler−Natta (Z−N) catalysts. With metallocene catalysis, the molar mass can be adjusted over a broad range and the polymers show a narrow molar mass distribution (MMD).[6] Highly tactic and tailored copolymers can be produced due to the stereo- and regiospecific nature of the catalysts.[7−9] Polymer chains containing a terminal vinyl group can be used as macro-comonomers, leading to the formation of long-chain branched (LCB) polymers.[10] The introduction of such macro-comonomers (produced either online or offline) leads to a distinctly higher LCB concentration.[11−14]

Single-site catalysts produce a novel combination of structures for LCB−PE with a narrow molar mass distribution, which was first reported in the patent literature in the mid-1990s.[15,16] Scientific papers covering this topic were published a few years later.[3,17] The first scientific proof of the formation of long-chain branches using metallocene catalysts was performed by a combination of SEC, NMR and rheology.[18]

Since then, many reports have revealed the high sensitivity of rheological measurements compared to the classical analytical methods for the detection of the LCBs in LCB−mPE.[5,18−23]

These developments are based on the following. Linear mHDPE and mLLDPE follow the exponential relationship of

$$\eta_0 = 9 \times 10^{-15} M_w^{3.6}, \quad \text{for } M_w > M_c \qquad (1)$$

between the zero shear-rate viscosity η_0 and the weight-average molar mass M_w. This relationship is valid for M_w larger than a critical molar mass M_c, and is independent of the molar mass distribution.[24] Furthermore, it is unaffected by the comonomer content of linear ethene/α-olefin copolymers (mLLDPEs) up to 30 wt % comonomer.[25−27]

The zero shear-rate viscosity η_0 of LCB−mPE lies distinctly above the η_0-M_w relation of linear samples when compared at the same absolute molar masses M_w.[2,6,19,28,29] This deviation from the η_0-M_w relation is often assessed by the zero shear-rate viscosity enhancement factor η_0/η_0^{lin}, with η_0^{lin} describing the zero shear-rate viscosity η_0 of a linear sample of the same molar mass M_w calculated from eq 1. Bersted[28] reported that η_0/η_0^{lin} goes through a maximum with increasing degree of long-chain branching at constant M_w. Highly branched samples of a different architecture, such as LDPE, lie below the η_0-M_w line,[21,28−32] but a low molecular LCB−mPE was found to lie below this threshold.[11,24] On the other hand, comb-like mPE with short arms can lie above the η_0-M_w relation.[14,33]

Besides η_0, the other terminal value, the linear steady-state elastic compliance J_e^0 is increased by the presence of long-chain branches,[21,22,34,35] whereas the plateau modulus is essentially not affected by the long-chain branches.[36] For LCB−mPE, an increase in J_e^0 from approximately 1×10^{-4} (lin. PE) to 30×10^{-4} was reported.[20−22,35] It was established qualitatively for

Received: March 10, 2011
Revised: May 26, 2011
Published: June 09, 2011

LCB−mPE that a higher branching level increases J_e^0 more than a lower one,[20,21,35] but there is insufficient data available to give more details on this issue. On the other hand, data on LDPE indicates that J_e^0 also goes through a maximum when considering it as a function of the long-chain branch content, taking into account that J_e^0 of LDPE is approximately at the same level as an LCB−mPE with an intermediate degree of long-chain branching.[24] In addition, the literature shows that the molar mass distribution and long-chain branches do not have additive effects, as J_e^0 of monodisperse stars is essentially the same as J_e^0 of LCB−mPE,[20,21,33,35] which is a mixture of linear and star-branched chains.[37] J_e^0 of the linear chains increases by at least 1 decade when going from monodisperse hydrogenated polybutadiene (which is essentially LLDPE) to mLLDPE.[5,26,33]

This study examined the correlations between the rheological quantities and molecular structure. A further intention is to establish a connection between the rheological quantities, which are relatively easy to measure, such as the critical phase angle δ_c, the intercept between the tangents laid through the turning points of $\delta(|G^*|)$, and those requiring considerable experimental effort. These correlations can then be used to make measurements of similar systems easier. In addition, the question as to whether the full range of shear rheological behavior of a grade can be predicted after only a few tests is addressed.

Table 1. Molecular data and zero shear-rate viscosities of the linear HDPE-samples (M-sh. means a shoulder in the molar mass distribution) used to establish the linear reference of the $\delta(|G^*|)$-plot

	M_w [g/mol]	M_w/M_n	M_z/M_w	η_0 [Pa s] (T = 150°C)	remarks
C1	42 000	3	2	520	low *M*-sh.
C3	120 000	2	1.6	17 800	
C4	224 000	3	1.7	113 200	high *M*-sh.
A4	564 000	4.3	2.1	6 732 310	

EXPERIMENTAL SECTION

Samples. The samples used in this paper have different origins. Most were synthesized by Prof. Kaminsky (University Hamburg).[6,19,20,38,39] Several other samples are from earlier projects. All samples were synthesized using metallocene catalysts. Some commercial samples have been produced by various polyolefin companies.

For the mHDPEs, Table 1 lists M_w, M_w/M_n, M_z/M_w, and the zero shear-rate viscosity η_0.

Tables 2, 3, and 4 list the zero shear-rate viscosity increase factor η_0/η_0^{lin}, the critical phase angle δ_c, and degree of long-chain branching from both SEC−MALLS and rheology for the LCB−mHDPEs (Table 2) and LCB−mLLDPEs (Tables 3 and 4).

All polyethylenes produced with *catalysts* B (rac-[Et(Ind)$_2$]ZrCl$_2$),D ([Me$_2$Si(Me$_4$Cp)N^{tert}Bu)]TiCl$_2$),E (Cp$_2$ZrCl$_2$), and F ([Ph2C(2,7-di^{tert}BuFlu)(Cp)]ZrCl$_2$) were synthesized by Kaminsky's group (Tables 2and 3).[6,20,41] MAO was used as a cocatalyst for all syntheses. In addition, two products of Gabriel[42] (LCB−mHDPE 1 and 2) and several LCB−mLLDPEs of Dow and Exxon (designated as LB*x*, where *x* is a consecutive number) are discussed in this paper (cf. Table 4).

LCB_R is the long-chain branching content determined from rheological indicators, which are discussed elsewhere.[6,20]

LCB_{SEC} is the long-chain branching content as determined from SEC−MALLS. It is taken as a qualitative indicator on how much coil contraction is found, i.e. approximately how many long-chain branches/molecule are present at high molar masses. The highest molar mass detectable by SEC−MALLS depends on the sample and is roughly factor 10 higher than M_w. Therefore, samples with a higher molar mass have more long-chain branches than lower molecular ones at the same degree of long-chain branching λ [LCB/10000 monomer]. Hence, LCB_{SEC} and λ differ in their quantification. Because of the coil contraction, quantification of the results is possible. However, the sensitivity is limited to radii of gyration $\langle r_g^2\rangle^{0.5}$ > 20 nm, which is approximately equivalent to M = 100 kg/mol for linear PE; and this limit for branched PE is even higher. Hence, only the highest fractions of the molar mass distribution of normal PE (typically M_w > 100 kg/mol) can be used for the LCB fraction, which means that any average degree of branching is limited to only a rather small fraction—namely the highest molar

Table 2. Rheological and Molecular Characteristics of the LCB−mHDPEs

	M_w [kg/mol]	MMD	η_0 (T = 150 °C) [Pa s]	η_0/η_0^{lin}	δ_c [deg]	LCB_R	LCB_{SEC}	λ [LCB/10000 monomer]
B2	93	1.9	8.7×10^5	126	35	significant	high	7
B4	100	2.0	6.6×10^5	73	37	significant	high	7
B5	67	2.1	4.2×10^3	2.0	68	very weak	none	≪1
B6	106	2.5	$>10^{8\,a}$	>9000	26	very significant	very high	9
B7	76	1.8	4.0×10^4	12	51	significant	high	5
B8	69	2.0	1.2×10^4	4.9	65	Weak	low	<1
B9	66	1.8	6.3×10^3	3.1	69	Weak	high	2
B10	66	2.1	3.2×10^3	1.6	71	very weak	none	≪1
B11	65	2.1	1.8×10^4	9.3	56	significant	high	4
B12	101	2.5	$\approx 2.0 \times 10^5$	17	38	very significant	very high	8
D1	1410	2.0	$>9 \times 10^{8a}$	>6.7	-	significant	none	≪1
D4	74	2.0	4.5×10^3	1.5	83	very weak	none	≪1
D5	365	2.6	$>9.0 \times 10^{6a}$	>12	-	very significant	high	3
E6	47	2.0	1.2×10^3	2.0	-	very weak	low	1
F1	102	2.0	3×10^4	3.1	72	Weak	high	1
F2	1150	4.0	$>10^{10}$	>169	-	very significant	low	0.2
F3/F0	173	2.0	4.4×10^5	6.8	63	significant	high	1
LCB−mHDPE 1[b]	128	2.2	3.7×10^5	25.3	41	significant	high	-
LCB−mHDPE 2[b]	109	2.3	3.1×10^5	16.9	46	significant	high	-

[a] η_{max} (no value for η_0 could be determined). [b] Data by Gabriel et al.,[35] SEC−MALLS data not suitable for comparison.

Table 3. Comonomer Content, Molecular, Thermodynamic, and Rheological Properties of the Laboratory Scale LCB−mLLDPEs.[19,20,38]

	comonomer [C_nH_{2n}]	n_c[a] [mol %]	w_c[b] [wt %]	T_m [°C]	T_c [°C]	ΔH [J/g]	x_c[c] [%]	M_w [kg/mol]	MMD	η_0 (T = 150 °C) [Pa s]	η_0/η_0^{lin}	δ_c [deg]	LCB_R	LCB_{SEC}	λ [LCB/10000 monomer]
B13P	3	n.d.	n.d.	n.d.	n.d.	n.d.	53	65	2.0	5.7×10^3	2.8	64.5	medium	-[e]	-[e]
F8A	8	1.1	4.3	120	100	128	44	240	2.1	1.2×10^6	5.8	64	significant	high	0.7
F8B	8	1.8	6.8	116	96	110	38	190	2.0	4.4×10^5	4.8	66	medium	medium	0.5
F10A	10	1.1	5.3	120	102	131	45	160	2.0	1.5×10^5	3.0	71	medium	high	0.5
F10B	10	1.7	8.0	116	97	93	32	170	2.0	1.4×10^5	2.3	76	weak	medium	0.3
F10C[d]	10	2.1	9.7	n.d.	n.d.	n.d.	n.d.	166	2.0	1.1×10^5	1.9	80	very weak	none	≪0.2
F12A	12	1	5.7	120	101	133	46	172	2.1	2.5×10^5	4.0	69	medium	high	0.6
F12B	12	1.7	9.4	116	96	99	34	160	2.0	1×10^5	2.0	78	weak	medium	0.2
F12C[d]	12	2.3	12.4	n.d.	n.d.	n.d.	n.d.	173	2.0	9.6×10^4	1.5	83	very weak	none	≪0.2
F18A	18	0.4	3.5	128	108	131	45	183	2.3	5.0×10^5	6.3	65	significant	high	0.6
F18B	18	1.5	12.1	117	98	110	38	167	1.9	1.6×10^5	2.9	76	weak	medium	0.3
F26A	26	0.5	6.1	129	106	136	47	185	2.1	4.5×10^5	5.5	66	significant	high	0.6
F26B	26	1.6	17.4	116	98	96	33	194	2.1	2.8×10^5	2.9	75	weak	medium	0.4

[a] comonomer content in *mol*% (determined by melt-state NMR[43,44]). [b] comonomer content in wt % [c] determined by WAXS,[45−47] [d] synthesized with a new batch of catalyst F, thus have slightly different properties compared to the samples synthesized with the old batch regarding the degree of long-chain branching.[19,20] The new batch has a higher activity and forms more long-chain branches because of the higher output that increases the concentration of the available macromers. [e] No reliable branching data available.

Table 4. Thermal and Molecular Characteristics of the Commercially Available LCB−mLLDPEs

	comonomer [C_nH_{2n}]	n_c[a,b] [mol %]	w_c[a,c] [wt %]	T_m [°C]	ΔH [J/g]	x_c [%]	M_w [kg/mol]	M_w/M_n	η_0 (T = 150 °C) [Pa s]	η_0/η_0^{lin}	δ_c[deg]	LCB_R	LCB_{SEC}	λ [LCB/10000 monomer]
LB1	8	5.9	20.1	101	97	33	94	2.2	4.2×10^4	6.3	64	significant	high	3
LB2	8	6.2	20.9	98	94	32	89	2.3	3.2×10^4	7.1	63	significant	high	3
LB3	8	2.6	9.6	112	88	30	85	1.9	3.8×10^4	9.8	56	significant	high	4
LB4	8	n.d.	n.d.	103	n.d.	n.d	85	2.3	5.1×10^4	13.1	58	significant	high	4
LB5	8	4.3	15.2	108	108	37	69	2.3	8.0×10^3	4.3	69	medium	medium	2

[a] Determined by FT-IR.[48] [b] Comonomer content in mol %. [c] Comonomer content in wt %.

mass fractions. Whether this fraction is representative to the total molar mass distribution is not easy to answer. The understanding of reaction kinetics for low degrees of long-chain branching states that it should be constant.[10,37] However, no experimental proof of this has been published so far for metallocene-catalyzed polyethylenes with a technologically relevant molar mass range to the best of the authors' knowledge.

Furthermore, there is no proof of the correctness of the Zimm−Stockmayer theory.[40] Hence, branching degrees determined with this theory are not 100% reliable. For the few cases where both direct quantification and SEC−MALLS were performed a reasonable agreement (±20%) was found.

The question how far the branching degree determined by the Zimm−Stockmayer theory[40] deviates from the real degree of long-chain branching, is not easy to answer. Because of the similarity of the branching structure of the samples, it can be safely assumed that the deviations between the measured values are systematic. For samples with very short long-chain branches, as can be synthesized by the macromer technique,[11,14] the deviation is significant, however. Hence, it is safe to assume that for regular LCB−mPE-samples—as discussed in this article—the long-chain branches are long enough that a molar mass dependence of the coil contraction is no longer present. For this reason, the degree of long-chain branching determined by SEC−MALLS can be considered to be reasonably reliable.

On the basis of this, the degree of long-chain branching can, be approximately quantified as an average branching level λ, measured in LCB/10000 monomers. The highest molar mass, at which a branching level can be determined, depends on M_w and because a constant branching level λ. Therefore, the more long-chain branches, the more coil contraction is present the higher the molar mass. For this reason, the quantification for low branching levels becomes the better the higher the molar mass for constant λ. For M_w below 120 kg/mol, an experimental error of 1−1.5 LCB/10000 monomer is found, for higher molar masses, the error is expected to be around 0.2 LCB/10000 monomer. The reason for the higher accuracy lies in the larger concentrations of polymer in the molar mass range, in which $\langle r_g^2 \rangle^{0.5}$ is detectable safely, and resulting from that the higher fraction of the molar mass distribution, in which $\langle r_g^2 \rangle^{0.5}$ can be assessed.

Two types of LCB−mLLDPE were characterized: several commercially available samples and samples synthesized with catalyst F[6,19,20,38] (except for B13P), varying distinctly more in their molecular composition than the commercial samples. The samples synthesized with cat. F are referred to "fluorenyl series".[19,20] The comonomer type and molar comonomer content n_c and weight content w_c are also given in Table 3 and 4, because the comonomer influences the thermal properties distinctly in these samples.

SEC−MALLS. Molar mass measurements were carried using a high temperature size exclusion chromatograph (Waters, 150C) equipped with refractive index (RI) and infrared (IR) (PolyChar, IR4) detectors. All measurements were taken at 140 °C using 1,2,4-trichlorobenzene (TCB) as the solvent. The high temperature SEC was coupled with a multi-angle laser light scattering (MALLS) apparatus (Wyatt, DAWN

EOS). Details of the experimental SEC−MALLS setup and measuring conditions are described elsewhere.[24]

The SEC−MALLS data are given in the tables as the weight-average molar mass M_w, polydispersity index M_w/M_n, and if applicable, the degree of branching calculated from the coil contraction according to the Zimm−Stockmayer theory.[40]

Melt State NMR, FT-IR and WAXD. The melt-state NMR was performed by K. Klimke, MPI Mainz, Germany, on a Bruker Advance 500 dedicated solid-state NMR spectrometer. The results are published in detail elsewhere.[20,44] The Fourier-Transform IR-spectroscopy measurements were performed using a Nicolet Magna 750-spectrometer.[48] The wide-angle X-ray diffraction measurements were obtained using a MiroMax007 diffractometer (Rigaku Denki Co. Ltd.) operated at 40 kV and 20 mA.[45−47]

Rheology. The samples were compression molded into circular discs of 25 mm in diameter and between 1 mm and 2 mm in height. Antioxidative stabilizers (0.5 wt % Irganox 1010 and 0.5 wt % Irgafos 38 (Ciba SC)) were added to the laboratory scale samples. The commercial samples were sufficiently stable without an additional stabilizer. More details are given elsewhere.[24]

Shear rheological tests were carried at a constant temperature of 150 °C in a nitrogen atmosphere. Most tests were carried out using a Bohlin/Malvern Gemini but some tests were also conducted using a Bohlin CSM, a Rheometric Scientific/TA Instruments ARES, and a TA Instruments AR-G2. The tests by Gabriel et al.[42] were performed using a self-built magnetic bearing rheometer.[49] Dynamic-mechanical tests (frequency sweeps) were carried out in the linear viscoelastic regime between frequencies ω of 1000 s^{-1} and 0.01 s^{-1}. Typically oscillatory stresses with amplitudes τ_0 between 10 and 100 Pa or deformation amplitudes γ_0 of approximately 5% were applied depending on the viscosity of the sample. The thermal stability was measured by conducting a frequency sweep after loading the sample and repeating the same test after longer creep and creep-recovery tests, which took up to 3 days per measurement. In some cases the thermal stability was extremely good, up to 2 weeks at 150 °C.

Creep and creep-recovery tests were performed to determine the zero shear-rate viscosity η_0 from the creep compliance $J(t')$ by

$$\log \eta_0 = \lim_{t' \to \infty} \left(\log \left(\frac{t'}{J} \right) \right) \quad (2)$$

The linear steady-state elastic compliance J_e^0 was determined from the elastic (creep-recovery) compliance $J_r(t)$ by

$$J_e^0 = \lim_{t, t' \to \infty} J_r(t) \quad (3)$$

The linearity and stationary nature was ensured for all creep and creep-recovery tests (for the precise methods and further experimental requirements to properly perform such tests see refs 50 and 51). Typically, creep stresses τ between 2 and 50 Pa were applied depending on the viscosity of the sample. If the terminal relaxation time was too long to reach the zero shear-rate viscosity η_0 or the linear steady-state elastic compliance J_e^0,[50−52] the acquired values were designated as η_{max} and J_e, respectively. In some cases, terminal values of J_e^0 were reached, but it was not possible to prove their linearity; these terminal values of $J_r(t)$ are also designated as J_e. η_{max} and J_e are always less than or equal to the terminal and linear values η_0 and J_e^0. Examples of creep and creep-recovery tests are given in Figure 1. For very long creep times, the creep compliance reaches a constant slope of 1, which is equal to a plateau in t'/J (eq 2). At very long recovery times, the elastic recoverable compliance $J_r(t)$ reaches a plateau, which is the *linear steady-state elastic compliance* J_e^0.

The relaxation spectra were calculated using the method reported by Stadler and Bailly.[54,55]

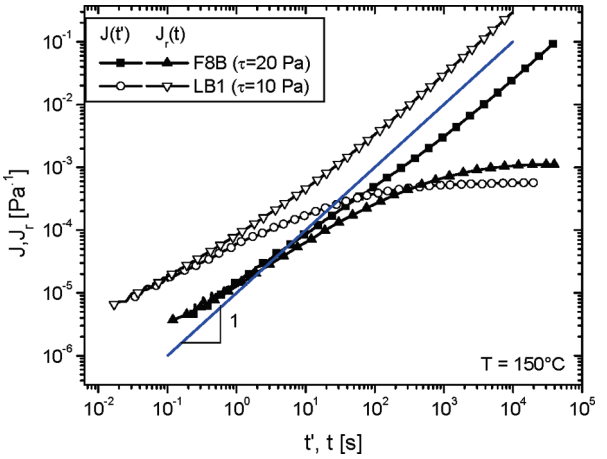

Figure 1. Examples of the creep and creep−recovery tests for samples F8B and LB1[53].

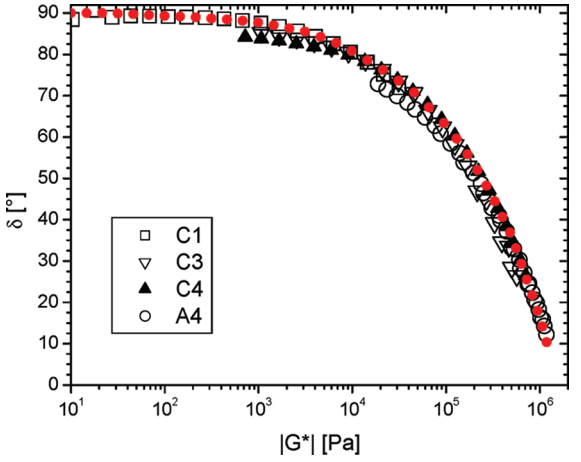

Figure 2. Plot of the linear references, C1, C3, C4, and A4.

RESULTS

***δ*(|*G**|) Plots.** One of the most successful ways of detecting long-chain branches is the $\delta(|G^*|)$ plot if linear and long-chain branched samples with the same molar mass distribution are compared.

Materials C1, C3, C4, and A4[6,24,39] were chosen as the linear standards, and are shown in Figure 2. The points fall on a line within the accuracy of the measurement.

Figure 3 shows $\delta(|G^*|)$ plots of several samples synthesized with *catalyst* B (*rac*-[Et(Ind)$_2$]ZrCl$_2$). Although the molar masses M_w of samples B7, B8, and B10 are similar (M_w of B6 is slightly higher), the deviation from the linear reference (dashed line) is significantly different for the samples shown. To quantify the deviation from the linear reference, the characteristic point p_c (∗ symbol) was defined by the intercept of the tangents to the turning points of the curves (☆ symbols).[56] p_c is described by $G_c$and δ_c, which will be discussed later in more detail.

δ_c decreases with increasing degree of long-chain branching. Although a high degree of branching was detected for B6, SEC−MALLS did not detect any LCBs for B10 (cf. Table 2). B7 and B8 are lightly branched.

Before being able to fully utilize the viscoelastic data for the characterization of the long-chain branches, it is important to

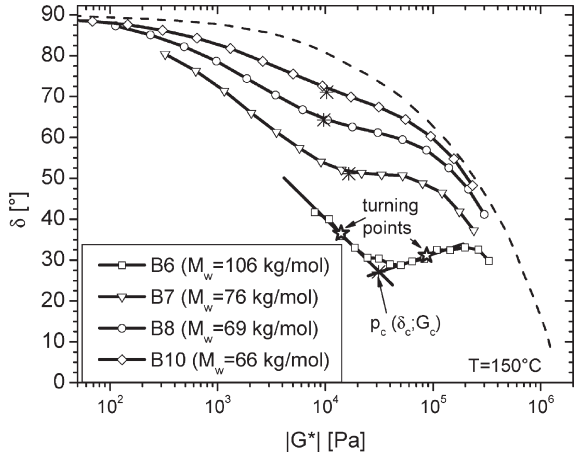

Figure 3. $\delta(|G^*|)$ plot of several samples synthesized with catalyst B. The dashed line is the linear reference (Figure 2).

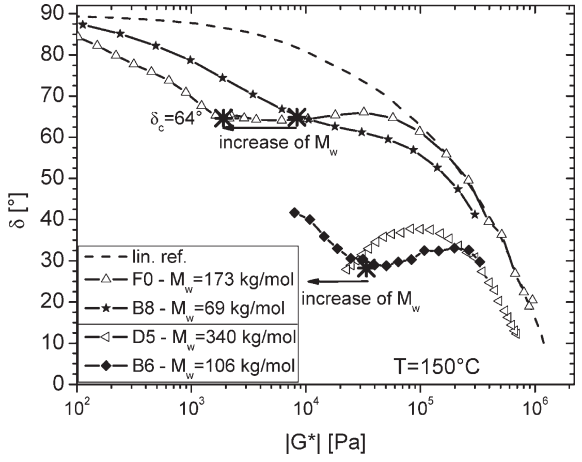

Figure 4. Characteristic coordinates p_c of the $\delta(|G^*|)$ plot of B6, B8, D5, and F0.

determine how other factors, namely the molar mass and molar mass distribution M_w/M_n of a sample, affects the viscoelastic behavior δ_c and G_c of long-chain branched samples.

Besides the characteristic phase angle δ_c, the x-coordinate of the characteristic point the complex modulus G_c shows a molar mass dependence.

This effect is shown in Figure 4 for δ_c of approximately 64° and 27° (even though δ_c could not be determined for D5). The higher molar mass of F0 than B8 leads to a shift of G_c toward lower values by a factor of approximately 5. Although, there is no 1:1 correlation, this ratio is the same as the change in ratio between the characteristic relaxation times λ_1 and λ_2, scaling with M_w with an exponent of 5.5 and 3.6, respectively.[57] The function $\delta(|G^*|)$ of B8 and F0 also differ distinctly in their shape. In the case of B8, the characteristic point p_c is determined only by a small bend, whereas F0 shows a plateau of δ of 1.8 decades in $|G^*|$. Therefore, it is much easier to determine p_c of F0 than B8.

B6 shows a small minimum in $\delta(|G^*|)$ leading to $\delta_c \approx 27°$. Sample D5 with an approximate triple molar mass M_w has approximately the same δ_c but at significantly lower $|G^*|$. This is a consequence of a very high M_w and a very long maximum relaxation time following from a high molar mass M_w and *long-chain branches*.

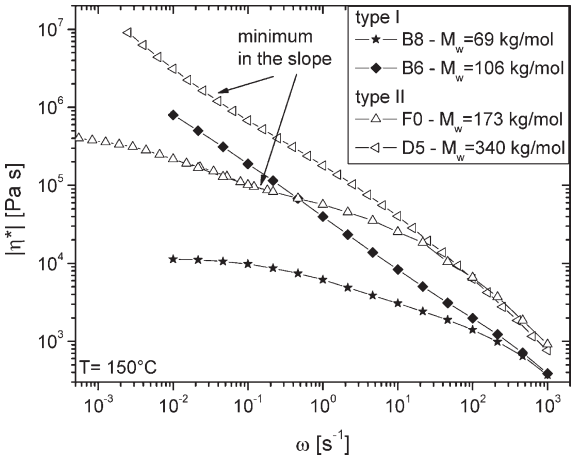

Figure 5. Viscosity functions $|\eta^*(\omega)|$ of B6, B8, D5, and F0.

The results indicate that the total number of long-chain branches per chain have an influence, which will be discussed later in more detail. It can also be concluded that two materials with same δ_c and MMD but different molar mass M_w will have a different G_c, which corresponds to different arm relaxation times.

Viscosity Functions. The different viscosity functions $|\eta^*(\omega)|$ can be classified into two different types by its shape, as shown in Figure 5. The group of *LCB−mPE viscosity functions* without a minimum and maximum in the slope are designated as *type I* and *type II*, respectively. At a low M_w (B8, B6), the viscosity function shows an approximately constant slope between these characteristic curvatures, whereas at higher M_w (F0, D5), the slope shows a minimum between the bends (marked by the arrows in Figure 5).

The introduction of *long-chain branches* into a melt leads to a change in the relaxation spectrum by the appearance of additional modes. The deviation of long-chain branched samples from the linear reference is caused by a second main mode, which is a consequence of LCB−mPE being a mixture of linear and long-chain branched chains, predominantly stars. The stronger molar mass dependence of the stars compared to the linear chains for arm molar masses $M_a \gtrsim 17$ kg/mol means that the ratio of the relaxation times of these two main modes increases with increasing molar mass. Therefore, the shape of the viscosity function $|\eta^*(\omega)|$ (and also of the other plots, such as $G'(\omega)$, $G''(\omega)$, and $\delta(|G^*|)$) changes with the molar mass.

In LCB−mPE, the two bends are visible (in the case of B8 (Figure 5) these bends are approximately $\omega = 300$ and 0.05 s^{-1}, and the low frequency bends of B6 and D5 are not reached). Nevertheless, the sample must possess such a high frequency bend because this bend corresponds to the transition of a double log slope between typically −0.1 and −0.8 to a high frequency value of −1, which corresponds to a constant modulus $|G^*(\omega)|$, and thus to the plateau modulus G_N^0, which all well entangled polymers must have.[58] *Type I* viscosity functions can be described successfully using the Carreau−Yasuda model extended by a second relaxation term,[63,64] in which two characteristic relaxation times, λ_1 and λ_2 can be assigned.[65,66] The characteristic relaxation time λ_2 is equivalent to the characteristic relaxation time λ from the Carreau−Yasuda model and scales with $M_w^{3.6}$, whereas λ_1 was attributed to the long-chain branches and scales with $M_w^{5.15}$.[57] Owing to the minimum in the slope of the viscosity function, it is not possible to fit the type II-viscosity functions with this model with acceptable accuracy.

This "two-dimensional" dependence of the linear viscoelastic behavior complicates the assessment without a model.

dx.doi.org/10.1021/ma200550c |*Macromolecules* 2011, 44, 5401–5413

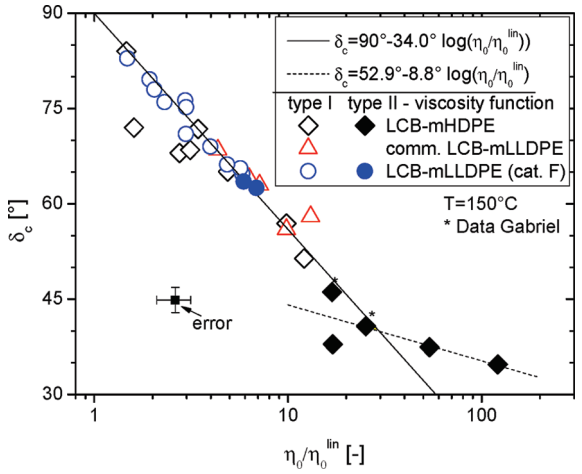

Figure 6. Critical phase angle δ_c as a function of the zero shear-rate viscosity enhancement factor η_0/η_0^{lin}. The error bars represent an error of ±20% with respect to η_0/η_0^{lin} stemming from the ±5% uncertainty in the determination of M_w by SEC−MALLS, δ_c can be determined with a reproducibility of approximately ±2°.

Correlation between the Characteristic Phase Angle δ_c and the Zero Shear-Rate Viscosity Enhancement Factor η_0/η_0^{lin}. A correlation can be found between the critical phase angle δ_c and *zero shear-rate viscosity enhancement factor* η_0/η_0^{lin} shown in Figure 6. The correlation is independent of the molar mass within the accessible range, where on one hand, a clear sign of a decrease of complex viscosity (with frequency) is present ($M_w \approx$ >60 kg/mol) but on the other hand, the maximum zero shear-rate viscosity η_0 (≈2 000 000 Pa s) has a maximum relaxation time still short enough to be measured by creep tests (t_0 = 100 000 s).

For δ_c > 40°, a linear correlation between the *zero shear-rate viscosity enhancement factor* η_0/η_0^{lin} and δ_c is found, which can be described as

$$\delta_c = 90°\left(1 - 0.378 \log\left(\frac{\eta_0}{\eta_0^{lin}}\right)\right)$$

$$= 90° - 34.02° \log\left(\frac{\eta_0}{\eta_0^{lin}}\right) \quad (4)$$

For η_0/η_0^{lin} > 20, the correlation fails. Only *type II viscosity functions* were found in this regime. Therefore, reaching such high zero shear-rate viscosity enhancements η_0/η_0^{lin} will decrease δ_c to a lesser extent than reduce η_0/η_0^{lin}. If the slope of the $\delta_c-\eta_0/\eta_0^{lin}$ relation does not change, theoretically, the maximum η_0/η_0^{lin} would be 442 (δ_c < 0° is physically impossible), which would pose a limitation without any physical relevance.

For higher molecular LCB−mHDPE samples with a *type II* viscosity function, another $\delta_c-\eta_0/\eta_0^{lin}$ relation was derived leading to

$$\delta_c = 52.9° - 8.8° \log\left(\frac{\eta_0}{\eta_0^{lin}}\right) \quad (5)$$

The two samples of the fluorenyl series with a type II viscosity function have only a very small minimum and hence agree with the $\delta_c-\eta_0/\eta_0^{lin}$ relation of eq 4.

Therefore, the distinct minimum in the $\delta-|G^*|$ plot leads to a significant increase in η_0/η_0^{lin}. This finding makes sense, because a minimum in δ means that the elasticity of a melt does not decrease monotonously with decreasing frequency (i.e., δ does not increase monotonously) but shows a small increase (just above δ_c in frequency), which is only visible in the case of significantly separated main relaxation times. Therefore, such materials have a drastically lengthened the terminal relaxation time. This increases η_0, but also leads to very long measurement times to reach η_0, which in many cases exceeds the thermal stability of the samples. For this reason, these samples could not be shown in Figure 6. Their (not terminal) data (i.e., η_{max}) suggests that η_0/η_0^{lin} is significantly higher than 30, which would be in the regime of the relation between δ_c and η_0/η_0^{lin} according to eq 5.

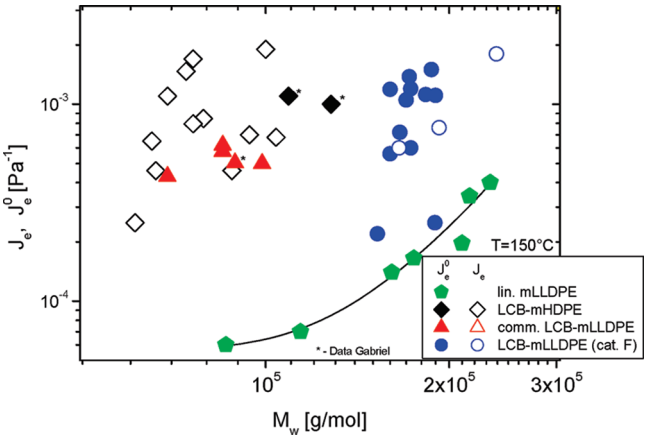

Figure 7. Plot of the linear steady-state elastic compliance J_e^0 (filled symbols) and steady-state elastic compliance J_e (open symbols) as a function of the molar mass M_w. A line was added to guide the eye.

This suggests that an increase in the "rheological effectiveness" of the *long-chain branches* (i.e., the increase of the LCB concentration or LCB length) is accompanied by a lengthening of the characteristic relaxation time λ_1 in relation to the molar mass M_w. This can be understood considering that mPE does not contain exclusively long-chain branched chains but also significant amounts of linear chains.[10,37,39]

A higher degree of branching leads to an increase in the average maximum relaxation time because the maximum relaxation time of long branched chains is much longer than that of a linear chain of equal molar mass. In addition, an increase in the degree of branching not only leads to fewer linear molecules but also to molecules with 2 or more LCBs/molecules, which have inner segments that are much more difficult to disentangle and have longer maximum relaxation time.

Linear Steady-State Elastic Compliance J_e^0. As the measurement of the linear steady-state elastic compliance J_e^0 (particularly the proof that the steady-state value of the elastic compliance J_e actually is J_e^0) requires numerous tests and very long measurement times, it was not possible to measure this quantity for all materials. In many cases, the thermal stability was insufficient or the necessary test time was simply too long, because one test would have exceeded several days (and often also the thermal stability of the sample).

For this reason, the nonstationary values J_e determined from $J_r(t)$ or viscoelastic data ($J'(\omega)$) were also used as an estimate of J_e^0. These nonstationary and/or nonlinear values need to be considered carefully because they are smaller than J_e^0. In many cases, it is possible that J_e^0 does not lie much higher by a comparison of the behavior of one sample to a similar one or by extrapolation of the functions recovery $J_r(t)$ or storage compliance $J'(\omega)$. Nevertheless, these values are only estimates and the scientific interpretation is, thus, limited.

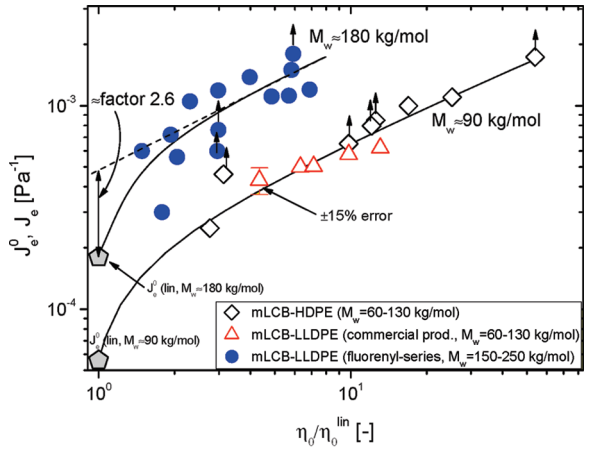

Figure 8. J_e^0 (or J_e) as a function of the zero shear-rate viscosity increase η_0/η_0^{lin}. The error bar is equal to ±15%.

As the melt elasticity is highly sensitive to the molar mass distribution,[42] only samples with $M_w/M_n \approx 2 \pm 0.2$ and without any high or low molecular tail are considered.

Before discussing the findings in detail, all the samples, whose zero shear-rate viscosity could be determined (thereby at least roughly fulfilling the stationarity criterion), and which were stable enough to at least obtain an estimate of J_e, are plotted in Figure 7 as a function of the molar mass M_w. The dependence of the elastic compliance on the molar mass $J_e^0(M_w)$ of linear mLLDPE is reported elsewhere.[26] The long-chain branched samples exhibit elastic compliances between 2×10^{-4} and 2×10^{-3} Pa^{-1}, which are distinctly higher than the values of the linear samples. Thus far, no LCB−mPE was found, which has a lower linear steady-state elastic compliance J_e^0 than that of the linear mLLDPE samples of the same molar mass distribution. This is in agreement with the findings for monodisperse, hydrogenated polybutadienes with different architectures.[33,67,68] The reason is that long-chain branches lead to a broadening of the relaxation spectrum in the terminal regime, which is equivalent to a higher J_e^0, as will be discussed in detail later.

No J_e^0-value was found for almost all the LCB−mHDPEs because most were synthesized with *catalyst* B, which produced samples with insufficient thermal stability to reach the stationary regime in creep recovery. The samples marked by the asterisk were obtained from Gabriel and Münstedt.[21]

The degree of long-chain branching determined by SEC−MALLS has too much error to be of any use for a quantitative discussion. Therefore, only the correlations between the elasticity and other rheological quantities are reasonable. Another problem of the SEC−MALLS is its high detection limit for *long-chain branches* (particularly at low molar masses M_w), which has been discussed in detail elsewhere.[69]

Correlation between the Linear Steady-State Elastic Compliance J_e^0 and the Zero Shear-Rate Viscosity Enhancement Factor η_0/η_0^{lin}. A plot of the linear steady-state elastic compliance J_e^0 (or J_e, if J_e^0 was not reached) as a function of the zero shear-rate viscosity increase, η_0/η_0^{lin} (Figure 8), shows that samples with different molar masses lie on different curves. This means that a lower molar mass M_w leads to a lower J_e^0 value (as a function of η_0/η_0^{lin}) for both linear and long-chain branched materials.

A comparison of the linear extrapolation (the dashed line in Figure 8 suggests its approximate shape) of the approximate functions of $J_e^0(\eta_0/\eta_0^{lin})$ (full lines in Figure 8) toward $\eta_0/\eta_0^{lin}=1$ (i.e., a linear chain) with the values for linear chains, the extrapolation lies above the measured values by a factor of 2−3 (shown for the fluorenyl series in Figure 8). Therefore, for very low degrees of long-chain branching, a significant increase in elasticity was found. This increase in melt elasticity is a good indicator for a very small degree of long-chain branching.

The distinct differences between J_e^0 for low and high molecular long-chain branched materials (open and filled symbols in Figure 8, respectively) was approximately a factor of 3, which is similar to that found for linear mLLDPE.[26] On the other hand, the reason for the increase in J_e^0 for linear mLLDPE is unclear. Several possibilities have been suggested but none could be proven or disproven. The most likely possibilities for the dependence of J_e^0 on the molar mass are the intrinsic dependence found only for polydisperse polymers because of the broader relaxation spectrum or the dependence of J_e^0 on the comonomer content.[26]

This can be understood from the finding that a higher M_w leads to overproportional lengthening of the terminal relaxation time for samples with a similar δ_c but different M_w exhibiting a different $|G^*|$ for the *x*-position of p_c (→shift of G_c, Figure 4). Because such an increase in the distance between the two main relaxation modes is basically a broadening of the relaxation spectrum, the linear steady-state elastic compliance J_e^0 increases (as it would also be a consequence of a broad MMD). As shown before, the zero shear-rate viscosity η_0 of linear samples is independent of the MMD, which means that a long-chain branched mPE with a higher molar mass M_w has a higher J_e^0 than a lower molecular one.[70]

To counter these relaxation spectrum width effects, a normalization of the elastic compliance J_e^0 to the elastic compliance of the linear sample of equal molar mass M_w $J_e^0(\text{lin})$, determined from the relationship between J_e^0 and M_w for mLLDPEs,[26] was performed, which is defined as follows:

$$J_e^0(\text{lin}) = J_{e0}^0 + c_1 \exp(M_w/c_2) \quad (6)$$

Here, $J_{e0}^0 = 3.33 \times 10^{-5}$ Pa^{-1}, $c_1 = 5.71 \times 10^{-6}$ Pa^{-1}, and $c_2 = 56027$ mol/g (its parameters do not have any physical meaning).

After molar mass normalization of the elastic compliance J_e^0 on the linear reference, the data of the LCB−mPE falls on one common "master curve" (the dashed line in Figure 9 suggests its approximate shape), which means that the elastic compliance is not only dependent on the branching structure itself but also on the molar mass of the sample, because M_w affects J_e^0 as well (eq 6). For $\eta_0/\eta_0^{lin} > 2$, this "master curve" can be described by the following equation:

$$\frac{J_e^0}{J_e^0(\text{lin})} = 3.78\left(\frac{\eta_0}{\eta_0^{lin}}\right)^{0.469} \quad (7)$$

which is given as the solid line in Figure 9.

Correlation between the Linear Steady-State Elastic Compliance J_e^0 and the Characteristic Phase Angle δ_c. The plot of $J_e^0/J_e^0(\text{lin})$ as a function of the critical phase angle δ_c also shows a linear relationship (Figure 10). However, no direct comparison of J_e^0 for a linear sample is possible due to the fact that δ_c is not defined for linear samples. Nevertheless, the complex modulus, at which the characteristic point $p_c(\delta_c, G_c)$ is found, corresponds to a phase angle of $\delta > 85°$ for linear polymers (with $M_w/M_n \approx 2$). A linear correlation between $J_e^0/J_e^0(\text{lin})$ and δ_c

$$\text{lin}\left(\frac{J_e^0}{J_e^0(\text{lin})}\right) = 2.06 - 0.018\delta_c \quad (8)$$

dx.doi.org/10.1021/ma200550c |*Macromolecules* 2011, 44, 5401–5413

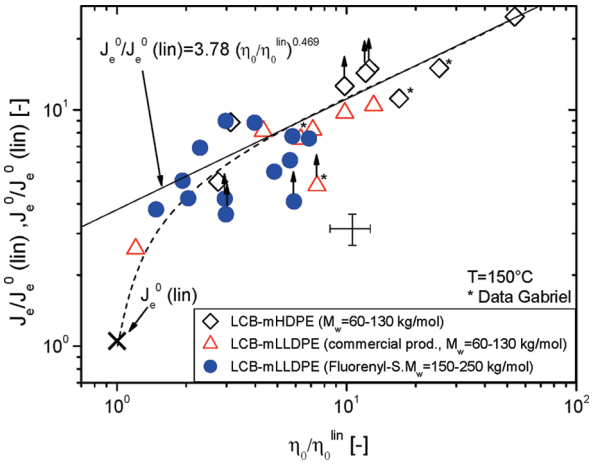

Figure 9. Normalized linear steady-state elastic compliance J_e^0/J_e^0 (lin) (or J_e/J_e^0 (lin)) as a function of the zero shear-rate viscosity enhancement factor η_0/η_0^{lin}. The error bars indicate an error of ±15% for the determination of J_e^0 and of ±20% for η_0/η_0^{lin}.

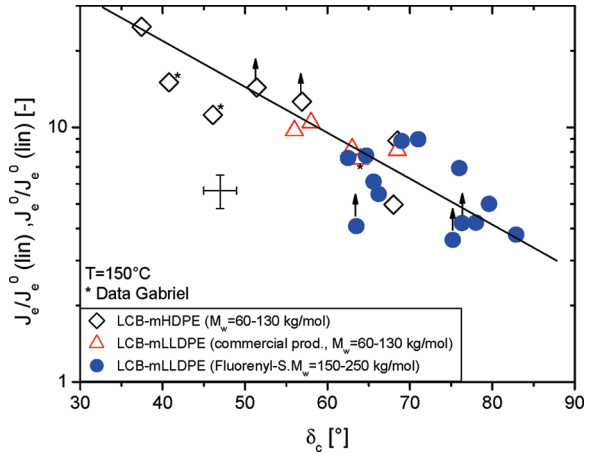

Figure 10. Normalized linear steady-state elastic compliance J_e^0/J_e^0(lin) (or J_e^0/J_e^0(lin)) as a function of the critical phase angle δ_c. The error bars indicate an error of ±15% for the determination of J_e^0 and ±2° for δ_c.

leads to J_e^0/J_e^0(lin) ≈ 3 for δ = 85°, which is similar to that found for J_e^0/J_e^0(lin) at η_0/η_0^{lin} = 1 (Figure 9).

This again shows that the correlation between δ_c, the slope between the main relaxation modes in the extended Carreau−Yasuda model, and η_0/η_0^{lin} can also be extended to J_e^0, which means that the quantities, which are difficult to measure (the zero shear-rate viscosity η_0 and linear steady-state elastic compliance J_e^0) can be deduced from the correlations between the different rheological quantities described here with sufficient accuracy.

Relation between Rheological Properties and Molecular Structure. Besides the molar mass M_w and the molar mass distribution (which is approximately constant for all samples discussed in this article) the most important molecular indicator of molecular structure is the branching content, which is discussed in terms of the branching frequency λ in units of LCB/10000 monomer, determined according to the Zimm−Stockmayer theory.[40] In general, the branching frequency λ should be a function of molar mass. Hence, giving the branching frequency, as a one single quantity is only possible due to the macromer

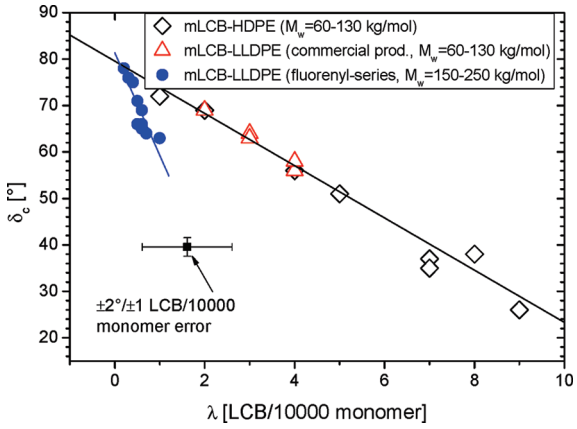

Figure 11. Relation between the critical phase angle δ_c and branching frequency λ. The error bars correspond to ±2° on the *y*-axis and ±1 LCB/10000 monomer on the *x*-axis.

process and intramolecular branching, which incorporates vinyl-terminated polymer chains as long-chain branches.[10,37,71] Piel et al.[6] and Stadler et al.[72] showed for long-chain branched PE that the long-chain branch frequency λ is roughly independent of molar mass. For the samples in this article—as far as λ was measurable—λ is approximately independent of molar mass *M*.

Figure 11 shows the relation between λ and δ_c for the samples with a molar mass M_w between 60 and 130 kg/mol and also between 150 and 250 kg/mol. Samples, for which the degree of long-chain branching could not be safely established, because it was too low, are omitted in Figure 11.

It is obvious that the samples fall on two linear relations. For the lower molecular samples, a relation with a slope of −5.6°/(LCB/10000 monomer) describes all the data within the experimental accuracy. For the high molecular "fluorenyl-series" a higher slope of −22.1°/(LCB/10000 monomer) is found to describe the data well.

On the basis of the relation established above, it is logical that also J_e^0/J_e^0(lin) and η_0/η_0^{lin} scale with λ.

The higher slope of the higher molecular samples can be explained by the fact that at constant λ, the average concentration of long-chain branches per sample depends on the weight-average molar mass M_w. Typically, the lower molecular series has a molar mass M_w of 80 kg/mol, while the higher molecular series has M_w≈170 kg/mol, which means that this series contains a more than twice as high LCB concentration.

In order to eliminate this influence, the molar mass M_w is multiplied with the degree of long-chain branching λ, which makes all samples roughly fall on one linear relation exhibiting a statistical scatter of about ±5° in δ_c. No systematic trend in the deviation could be detected (such as the one for the relation between J_e^0 and η_0/η_0^{lin}).

DISCUSSION

The relations established above can be summarized by three statements:

1. Zero shear-rate viscosity η_0 and steady-state elastic recovery compliance J_e^0 are increased by the introduction of long-chain branches. For better visualization, these quantities are normalized to their linear counterparts
2. A more or less pronounced minimum in the phase angle is observed, which can be quantified by the characteristic

phase angle δ_c. Its "pronouncedness" increases with increasing molar mass and level of long-chain branching.

3. δ_c, η_0 and J_e^0 can be related to each other. The correlations of J_e^0 and η_0 with the other quantities, however, are only possible after normalization of linear samples with equal M_w (J_e^0(lin) and η_0^{lin}, respectively). For J_e^0, the requirement for normalization is rather unexpected.

This raises the question as to what causes these correlations.

To answer this, the following question needs to be answered: How is the molecular structure of a LCB−mPE made up and on which parameters does it depend?

MOLECULAR STRUCTURE OF LCB−MPE

Soares and Hamielec[10] reported that the LCB formation mechanism of LCB−mPE is terminal branching. In terminal branching, vinyl terminated chains (macromonomers) insert into the growing chain. This process is comparable to the production of random copolymers and differs only from this by the much lower content of the much higher molecular macromonomer than a typical comonomer. This "intermolecular macromer incorporation" is a widely accepted mechanism. Nevertheless, there are many experimentally observed trends, particularly for slurry and gas phase polymerizations, which cannot be explained by this mechanism.[71] For example, B10 was produced under the same conditions as B6, except for a higher polymerization temperature. On the basis of the terminal branching mechanism, the probability of vinyl ended chain production is high. Consequently, the LCB content must be higher for B10 but B6 has a higher degree of LCB. This phenomenon was also observed for E3 and E6.

Therefore, a new "intra-molecular macromer incorporation" mechanism was proposed by Yang et al..[71] They stated that the previously produced chain with vinyl end remains attached to the active site during subsequent chain growth, and can act as a macromer that becomes incorporated on a growing chain as a LCB. On the basis of this explanation, the high molecular weight part of a polymer, contains longer branches.

Costeux et al.[37] established a model to describe the reaction mechanism based on the random incorporation of vinyl-terminated chains. Because the structure of LCB−PE produced via inter- and or intramolecular macromer incorporation approaches[10,71,73] are similar, and only the long-chain branching contents differ, an approximation of the structure of LCB−mPE can be drawn.

The discussion above suggests that an LCB−mPE is roughly comprised of three components:

1. Linear chains with M_w slightly smaller than M_w^{total},
2. Star-like chains with $M_w \approx 3M_n^{total}$ (=1.5 M_w^{total})
3. Higher branched chains, typically comb-like with a linear or star-like backbone with $M_w \gg M_w^{total}$.

These three components exist in various ratios. Higher-branched chains are significantly rarer than star-like chains as long as no extra macro-monomer is introduced and the degree of long-chain branching is rather low. According to Costeux et al.,[37] the concentration of higher branched chains is approximately one-third of the star-like species with not too high levels of long-chain branching.

On the basis of these theories,[10,37] the average number of LCB/molecule m should be theoretically sufficient for the characterization of LCB−mPE. The universality of the $\delta_c(M_w \times \lambda)$ relation (Figure 12) is a good indicator that this finding is true within the accuracy of the experiment.

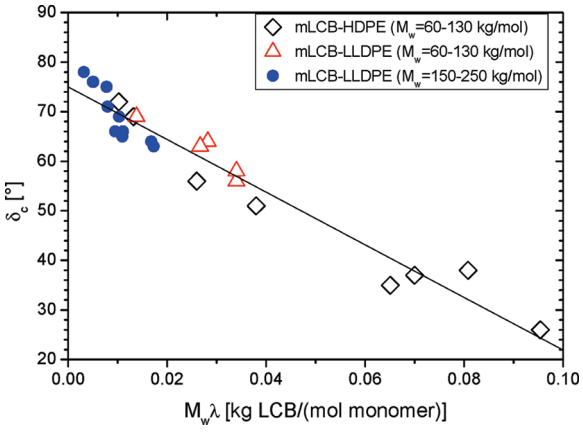

Figure 12. relation between the critical phase angle δ_c and weight-average molar mass multiplied with branching frequency $M_w \times \lambda$.

RHEOLOGICAL BEHAVIOR

Literature Data on Model Branched Polymers. *Star Polymers.* Star polymers are the simplest long-chain branching structure imaginable consisting only of one branching point with 3 or more branches originating from it. The rheological behavior of stars shows $\eta_0/\eta_0^{lin} <$ 1 for small molar masses (→ short arms) and >1 for high molar masses.[33,67,74−81] Gabriel[42] reported for these different systems that η_0/η_0^{lin} as a function of M/M_e is independent of the polymer type, and depends only on the number of arms, f, per molecule (thus $\eta_0/\eta_0^{lin}(M/(M_e \times f))$ is universal).

Pearson and Helfand[82] derived the equation

$$\eta_0 \propto \left(\frac{M_a}{M_e}\right)^{\alpha} \exp\left(\nu'\frac{M_a}{M_e}\right) \qquad (9)$$

to describe the correlations between η_0 and M, where M_a is the arm length, M_e the entanglement molar mass, $\alpha \approx 1$ and $\nu' \approx$ 0.5. This theoretical description was refined later[83] based on the tube model.[83−85] The viscosity and modulus functions of the star polymers were found to be quite similar to linear polymers in shape but exhibited a wider transition area, which is related to the increase in linear steady-state elastic compliance J_e^0 by a factor of approximately 20 compared to linear monodisperse samples.[33]

Comb and Pom-Pom Polymers. Few data for pom-poms exist, which have yielded some insight into their rheological behavior.[86−89] A special class of pom-poms, which are somewhat easier to synthesize, have only two arms per branch point, known as H-polymers.[88,90−97] The pom-pom-model[83] is generally considered to be valid for describing the linear rheological properties of this class of polymers.

Comb polymers are defined as having a single backbone with a length (in entanglements) with q arms attached, where the chain ends of the backbone also count as arms from their last branching point.[33,88,92,93] For monodisperse comb polymers, Inkson et al.[98] found an approximate relationship between the molar mass M and zero shear-rate viscosity η_0. The correlation between the zero shear-rate viscosity η_0 and molar mass M_w for both pom-pom and combs exceeded the η_0-M_w-correlation for three-arm stars in the case of two branches per molecule,[33] which is in agreement with the comb-model.

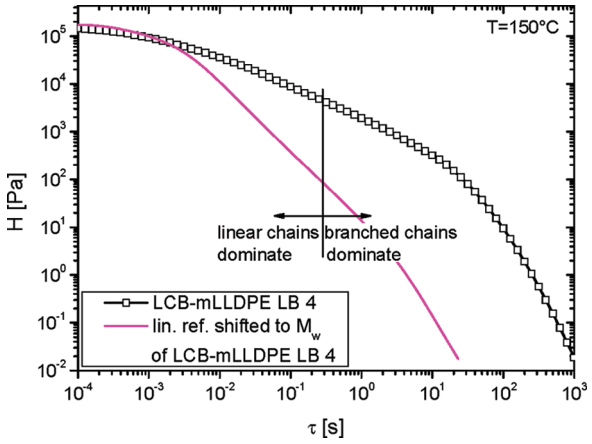

Figure 13. Comparison of the spectra of *long-chain branched* LB 4 and the linear reference, average of the spectra of 6 LLDPE, normalized by molar mass.

One problem regarding the characterization of long-chain branched chains is obvious from the model polymers. The maximum relaxation time τ_d is always increased distinctly compared to linear samples with the same M. The molecular reason for this lies in the fact that the reptation which only linear chains are capable of is faster for medium or highly entangled systems[99] than the fluctuation processes that all types of chains can undergo. Therefore, the full spectrum is much broader (as well as the necessary measurement time regime for capturing it) for long-chain branched polymers than for linears.

McLeish[101] has given an overview of the methods to modeling the rheological data of such model architectures.

Conclusions for LCB−mPE. The rheological data for monodisperse star and comb model polymers clearly shows that the terminal relaxation time of branched polymers is significantly higher than that for linear ones, provided all the segments are well entangled.[33,98,102] A shorter terminal relaxation time (and thus a lower η_0 than for linear samples of equal molar mass) is found only for combs or trees with very short arms.

The polydispersity will change these relationships somewhat because unlike linear samples, the relationship between the terminal relaxation time and molar mass of star-like polymers is exponential rather than a power law (linear polymers).

Therefore, when assuming a double logarithmic mixing law,[103] which is approximately fulfilled in many cases, a broadening of the molar mass distribution at constant M_w leads to an increase in the zero shear-rate viscosity η_0 and terminal relaxation time τ_d.

The typical LCB−mPE is a mixture of linear, star-like and higher branched molecules. With the exception of the very highly branched samples (e.g., B12), branched molecules comprise only a small fraction of chains. For this reason, it is logical that such samples also show the characteristics of linear samples, as indicated in the relaxation spectra in Figure 13. The spectrum for linear polymers,[104] adjusted to the M_w of the LCB−mLLDPE LB4 resembles closely the characteristics of LB4 for $\tau<10^{-2}$ s, i.e., for the highest frequencies. For longer relaxation times (lower frequencies), however, the curves disagree. This becomes more pronounced at longer relaxation times.

These higher relaxation strengths are clearly a trace of the long-chain branches, which introduce long-time modes. The spectrum differs significantly according to the materials but the general pattern (agreement with the linear reference for short relaxation times and deviation to higher relaxation strengths at long relaxation times) is present for all samples.

These differences in the relaxation spectra can be related to the zero shear-rate viscosity increase factor, η_0/η_0^{lin}, and the steady-state elastic recovery compliance J_e^0, as both quantities are integrals of the spectrum (eqs 11 and 12 refer to the continuous and discrete spectra, respectively):

$$\eta_0 = \int_{-\infty}^{\infty} H(\tau)\tau \, d(\ln \tau) = \sum_{i=1}^{n} g_i \tau_i \qquad (11)$$

$$J_0^e = \frac{\int_{-\infty}^{\infty} H(\tau)\tau^2 \, d(\ln \tau)}{\left(\int_{-\infty}^{\infty} H(\tau)\tau^2 \, d(\ln \tau)\right)^2} = \frac{\sum_{i=1}^{n} g_i \tau_i^2}{\left(\sum_{i=1}^{n} g_i \tau_i\right)^2} \qquad (12)$$

Therefore, it is logical that the dependencies of η_0/η_0^{lin} and J_e^0/J_e^0 (lin) correspond to each other, as their spectra have approximately the same shape.

δ_c is more difficult to obtain from the spectrum. On the basis of the Kramers−Kronig relations, the slope of the spectrum $H(\tau)$ or of the viscosity function $|\eta^*(\omega)|$ in log−log scaling is roughly related to δ_c. The validity of the relation has been demonstrated indirectly by finding direct relationships between η_0/η_0^{lin} and n, i.e., the slope between the main relaxation times λ_1 and λ_2 in the modified Carreau-Yasuda-model, and the relationship between n and δ_c.[57,65,66]

The molecular meaning of the relationships between δ_c, η_0/η_0^{lin} and J_e^0/J_e^0(lin) lies in the following:

1. The quantities react similarly to changes in molecular structure so that it is possible to find simple correlations between them.
2. In the range of molar masses accessible by rheological quantities, the molar mass has an effect, which can be normalized by the relationships between the molar mass and η_0 and J_e^0 for linear samples.

These relationships are valid despite the finding that the $\delta(|G^*|)$ plot shows a clear molar mass dependence, which was also found for the λ_1-M_w and λ_2-M_w relations, which have different slopes and can lead to a molar mass dependent ratio.[57]

Overall, with the establishment of the relationships between δ_c, η_0/η_0^{lin} and J_e^0/J_e^0(lin) it is sufficient to measure one of these quantities to determine the others with reasonable accuracy. Obviously, δ_c is the easiest of the three quantities to measure. For this reason, it is suggested to determine only δ_c and then estimate η_0 and J_e^0 from the relationships discussed in this article. This will save approximately 90% of the measurement time.

The fact that δ_c correlates very well with $\lambda \times M_w$, which can be considered as a quantity proportional to the number of long-chain branches at a characteristic molar mass (e.g., M_w), is a good indicator that δ_c is only influenced by the concentration of long-chain branches present in the material (in terms of average number of LCB/molecule—expressed by $\lambda \times M_w$) and that their length or the molar mass of the total polymer does not play a significant influence. As established before, J_e^0 is influenced by molar mass, which is why a correlation between δ_c and J_e^0 only works for J_e^0 normalized on the linear reference.

Self-evidently, the $\delta_c(\lambda \times M_w)$ correlation implies that the same correlation is also present for $\eta_0/\eta_0^{lin}(\lambda \times M_w)$ (cf. Figures 6 and 12). Nevertheless, this correlation is surprising. On the basis of eq 9

and also on the more complicated comb-model,[98] it is expected that a longer long-chain branch should increase the zero shear-rate viscosity increase factor η_0/η_0^{lin}. Such longer long-chain branches are expected to be formed by the macromer long-chain branch formation mechanism[10] when increasing with molar mass M_w for constant MMD M_w/M_n and $\lambda \times M_w$.

Giving a definite reason for this deviation between theory and measurement is not possible. There are several possible reasons:

1. The degree of long-chain branching of the higher molecular fluorenyl series is rather small, so that the molar mass dependence cannot be detected, as not enough long-chain branches are present.
2. The range of molar masses covered by the $\delta_c(\lambda \times M_w)$ relation is not sufficient for finding a distinct M_w dependence of $\delta_c(\lambda \times M_w)$.
3. An increase in molar mass of the vinyl-terminated potential LCBs reduces the likeliness of their incorporation into the growing chain, as their solubility in the solvent toluene used for the polymerization is decreased distinctly. Hence, preferably shorter macromers are incorporated into the growing chain. Therefore, the average long-chain branch length does not increase proportional to M_w but only mildly increases.

Possibility 2 is hard to judge: an increase of η_0/η_0^{lin} of an ideal symmetric star by factor >1000 between M_w = 65 kg/mol and 200 kg/mol is found, which, however, might not be enough to unravel the disagreement. Because not all chains in LCB−mPE are symmetric stars, such a disagreement might be concealed. To this end, it is impossible to judge whether possibility 2 is true or not.

Possibility 3—the preferred incorporation of shorter macromers due to their better solubility—probably plays a role, too. This can be seen from the fact that the higher the molar mass M_w of the sample, the lower the degree of long-chain branching. However, it is impossible to judge this effect quantitatively, as the length of the long-chain branches cannot be measured individually.

As the samples of the fluorenyl series LCB−mPEs in Figure 12 show a trend having a somewhat higher slope than the lower molecular LCB−mPEs, it is likely that possibility 1 plays a role. This, however, does not mean that possibility 2 and 3 are irrelevant.

SUMMARY

η_0/η_0^{lin} and δ_c are related to each other but for the *type II viscosity functions*, which have a $\delta_c < 45°$ the relationship established for materials with a *type I* viscosity function is replaced by another linear correlation with a much smaller slope.

Unlike the correlation between η_0/η_0^{lin} and δ_c, no molar mass independent correlation was found for J_e^0. This is a consequence of the elastic properties being strongly dependent on the molecular structure, more distinctly than the viscous properties. Therefore, only a molar mass dependent relationship between η_0/η_0^{lin} and the elastic compliance J_e^0, i.e. $J_e^0/J_e^0(\text{lin})$ leads to a "master curve" for the increase in this quantity with increasing degree of branching.

An indication for a universality in the relation between δ_c and η_0/η_0^{lin} on one hand and the branching frequency $\lambda \times M_w$ on the other hand was found.

AUTHOR INFORMATION

Corresponding Author

*E-mail: fjstadler@jbnu.ac.kr. Telephone: +82 63 270-4039. Fax: +82 63 270-2306.

ACKNOWLEDGMENT

The authors wish to thank the German Research Foundation (DFG), "Human Resource Development (Advanced track for Si-based solar cell materials and devices; project number 201040100660)" of the Korea Institute of Energy Technology Evaluation and Planning (KETEP) grant funded by the Korea government Ministry of Knowledge Economy, and Ministry of Science, Research and Technology of Iran for the financial support. Discussions with Prof. Dr. Helmut Münstedt, Friedrich-Alexander University have greatly contributed to the understanding presented in this work. In addition, the contributions of Mrs. I. Herzer and Dr. J. Kaschta (Erlangen) regarding the SEC−MALLS measurements, of Prof. Dr. W. Kaminsky and Dr. C. Piel (University Hamburg) with respect to the synthesis of many of the samples in this article, and of Dr. K. Klimke and Dr. M. Parkinson from the Max-Planck Institute of Polymer Research in Mainz concerning the solid state NMR-measurements are gratefully recognized. The help of Mrs. M. Sturm (Erlangen) for the FT-IR measurements are also appreciated.

REFERENCES

(1) Bubeck, R. A. *Mater. Sci. Eng.* **2002**, *R 39*, 1–28.
(2) Wood-Adams, P. M.; Dealy, J. M. *Macromolecules* **2000**, *33*, 7481–7488.
(3) Malmberg, A.; Kokko, E.; Lehmus, P.; Löfgren, B.; Seppälä, J. *Macromolecules* **1998**, *31* (24), 8448–8454.
(4) Lehmus, P.; Kokko, E.; Harkki, O.; Leino, R.; Luttikhedde, H.; Nasman, J.; Seppälä, J. *Macromolecules* **1999**, *32* (11), 3547–3552.
(5) Gabriel, C.; Münstedt, H. *Rheol. Acta* **1999**, *38* (5), 393–403.
(6) Piel, C.; Stadler, F. J.; Kaschta, J.; Rulhoff, S.; Münstedt, H.; Kaminsky, W. *Macromol. Chem. Phys.* **2006**, *207* (1), 26–38.
(7) Resconi, L.; Cavallo, L.; Fait, A.; Piemontesi, F. *Chem Rev* **2000**, *100* (4), 1253–1345.
(8) Heuer, B.; Kaminsky, W. *Macromolecules* **2005**, *38* (8), 3054–3059.
(9) Coates, G. W. *Chem Rev* **2000**, *100* (4), 1223–1252.
(10) Soares, J. B. P.; Hamielec, A. E. *Macromol. Theory Simul.* **1996**, *5* (3), 547–572.
(11) Arikan, B.; Stadler, F. J.; Kaschta, J.; Münstedt, H.; Kaminsky, W. *Macromol. Rapid Commun.* **2007**, *28* (14), 1472–1478.
(12) Rulhoff, S.; Kaminsky, W. *Macromol. Symp.* **2006**, *236*, 161–167.
(13) Peruch, F.; Lahitte, J. F.; Isel, F.; Lutz, P. J. *Macromol. Symp.* **2002**, *183*, 159–164.
(14) Stadler, F. J.; Arikan-Conley, B.; Kaschta, J.; Kaminsky, W.; Münstedt, H. *Macromolecules* **2011**, 10.1021/ma200588r.
(15) Lai, S. Y.; Wilson, J. R.; Knight, G. W.; Stevens, J. C.; Chum, P. W. S. *Elastic substantially linear olefin polymers*. U.S. Patent 5,272,236, 1993.
(16) Brant, P.; Canich, J. A. M.; Dias, A. J.; Bamberger, R. L.; Licciardi, G. F.; Henrichs, P. M. *Long-chain branched polymers and a process to make long-chain branched polymers*. WO 94/07930, 1994.
(17) Harrison, D.; Coulter, I. M.; Wang, S. T.; Nistala, S.; Kuntz, B. A.; Pigeon, M.; Tian, J.; Collins, S. *J. Mol. Catal. A: Chem.* **1998**, *128* (1−3), 65–77.
(18) Wood-Adams, P. M.; Dealy, J. M.; deGroot, A. W.; Redwine, O. D. *Macromolecules* **2000**, *33* (20), 7489–7499.
(19) Stadler, F. J.; Piel, C.; Kaminsky, W.; Münstedt, H. *Macromol. Symp.* **2006**, *236* (1), 209–218.
(20) Stadler, F. J.; Piel, C.; Klimke, K.; Kaschta, J.; Parkinson, M.; Wilhelm, M.; Kaminsky, W.; Münstedt, H. *Macromolecules* **2006**, *39* (4), 1474–1482.
(21) Gabriel, C.; Münstedt, H. *Rheol. Acta* **2002**, *41* (3), 232–244.
(22) Malmberg, A.; Gabriel, C.; Steffl, T.; Münstedt, H.; Löfgren, B. *Macromolecules* **2002**, *35*, 1038–1048.

(23) Kokko, E.; Wang, W.; Seppälä, J.; Zhu, S. *J. Polym. Sci., Part A: Polym. Chem.* **2002**, *40* (19), 3292–3301.
(24) Stadler, F. J.; Piel, C.; Kaschta, J.; Rulhoff, S.; Kaminsky, W.; Münstedt, H. *Rheol. Acta* **2006**, *45* (5), 755–76410.1007/s00397-005-0042-6.
(25) Wood-Adams, P. M. *The effect of long chain branching on the rheological behavior of polyethylenes synthesized using constrained geometry and metallocene catalysts*. McGill-University: Montreal, Canada, 1998.
(26) Stadler, F. J.; Münstedt, H. *J. Rheol.* **2008**, *52* (3), 697–712.
(27) Utracki, L. A.; Schlund, B. *Polym. Eng. Sci.* **1987**, *27* (5), 367–79.
(28) Bersted, B. H. *J. Appl. Polym. Sci.* **1985**, *30*, 3751–3765.
(29) Auhl, D.; Stange, J.; Münstedt, H.; Krause, B.; Voigt, D.; Lederer, A.; Lappan, U.; Lunkwitz, K. *Macromolecules* **2004**, *37* (25), 9465–9472.
(30) Münstedt, H.; Gabriel, C.; Auhl, D. *Abstr. Pap. Am. Chem. Soc.* **2003**, *226*, U382–U382.
(31) Stange, J.; Uhl, C.; Münstedt, H. *J. Rheol.* **2005**, *49*, 1059–1080.
(32) Laun, H. M.; Münstedt, H. *Verhandlungen DPG VI* **1983**, *18*, 53.
(33) Lohse, D. J.; Milner, S. T.; Fetters, L. J.; Xenidou, M.; Hadjichristidis, N.; Roovers, J.; Mendelson, R. A.; Garcia-Franco, C. A.; Lyon, M. K. *Macromolecules* **2002**, *35* (8), 3066–3075.
(34) Plazek, D. J.; Echeverria, I. *J. Rheol.* **2000**, *44* (4), 831–84110.1122/1.551117.
(35) Gabriel, C.; Kokko, E.; Löfgren, B.; Seppälä, J.; Münstedt, H. *Polymer* **2002**, *43* (24), 6383–6390.
(36) Wood-Adams, P. M. *J. Rheol.* **2001**, *45* (1), 203–210.
(37) Costeux, S.; Wood-Adams, P.; Beigzadeh, D. *Macromolecules* **2002**, *35*, 2514–2528.
(38) Kaminsky, W.; Piel, C.; Scharlach, K. *Macromol. Symp.* **2005**, *226* (1), 25–34.
(39) Stadler, F. J.; Kaschta, J.; Münstedt, H. *Macromolecules* **2008**, *41* (4), 1328–133310.1021/ma702367a.
(40) Zimm, B. H. M.; Stockmayer, W. H. *J. Chem. Phys.* **1949**, *17* (12), 1301–1314.
(41) Stadler, F. J.; Gabriel, C.; Münstedt, H. *Macromol. Chem. Phys.* **2007**, *208* (22), 2449–2454.
(42) Gabriel, C., *Einfluss der molekularen Struktur auf das viskoelastische Verhalten von Polyethylenschmelzen*; Shaker-Verlag: Aachen, Germany, 2001; Vol. Ph.D.
(43) Pollard, M.; Klimke, K.; Graf, R.; Spiess, H. W.; Wilhelm, M.; Sperber, O.; Piel, C.; Kaminsky, W. *Macromolecules* **2004**, *37* (3), 813–825.
(44) Klimke, K.; Parkinson, M.; Piel, C.; Kaminsky, W.; Spiess, H.-W.; Wilhelm, M. *Macromol. Chem. Phys.* **2006**, *207* (4), 382–395.
(45) Stadler, F. J.; Takahashi, T.; Yonetake, K. *e-Polym.* **2009**, 40.
(46) Stadler, F. J.; Takahashi, T.; Yonetake, K. *e-Polym.* **2009**, 41.
(47) Stadler, F. J.; Takahashi, T.; Yonetake, K. *Eur. Polym. J.* **2011**, *47* (5), 1048–1053.
(48) Stadler, F. J.; Kaschta, J.; Münstedt, H. *Polymer* **2005**, *46* (23), 10311–10320.
(49) Link, G.; Schwarzl, F. R. *Rheol. Acta* **1985**, *24* (3), 211–219.
(50) Gabriel, C.; Kaschta, J. *Rheol. Acta* **1998**, *37*, 358–364.
(51) Gabriel, C.; Kaschta, J.; Münstedt, H. *Rheol. Acta* **1998**, *37* (1), 7–20.
(52) Wolff, F.; Resch, J. A.; Kaschta, J.; Münstedt, H. *Rheol. Acta* **2010**, *49* (1), 95–10310.1007/s00397-009-0396-2.
(53) Resch, J. A.; Stadler, F. J.; Kaschta, J.; Münstedt, H. *Macromolecules* **2009**, *42* (15), 5676–5683.
(54) Stadler, F. J.; Bailly, C. *Rheol. Acta* **2009**, *48* (1), 33–4910.1007/s00397-008-0303-2.
(55) Stadler, F. J. *Rheol. Acta* **2010**, *49* (10), 1041–1057.
(56) Trinkle, S.; Walter, P.; Friedrich, C. *Rheol. Acta* **2002**, *41* (1−2), 103–113.
(57) Stadler, F. J.; Münstedt, H. *Macromol. Mater. Eng.* **2009**, *294* (1), 25–34.
(58) Typically, a clear plateau modulus is found for $M_w > 10 \times M_e$ (M_e is the entanglement molar mass).[59−61] All samples discussed in this paper are well entangled because M_e of PE is approximately 800 g/mol[62] and the lowest molecular sample (C1) has a molar mass of 42,000 g/mol.
(59) Schausberger, A. *Rheol. Acta* **1991**, *30* (2), 197–202.
(60) Liu, C. Y.; Halasa, A. F.; Keunings, R.; Bailly, C. *Macromolecules* **2006**, *39* (21), 7415–7424.
(61) Liu, C. Y.; He, J. S.; van Ruymbeke, E.; Keunings, R.; Bailly, C. *Polymer* **2006**, *47* (13), 4461–4479.
(62) Fetters, L. J.; Lohse, D. J.; Colby, R. H. Chain Dimensions and Entanglement Spacings. In *Physical Properties of Polymers*, 2nd ed., Mark, J. E., Ed.; Springer: Heidelberg, Germany, 2007.
(63) Carreau, P. J. *Trans. Soc. Rheol.* **1972**, *16* (1), 99–127.
(64) Yasuda, K.; Armstrong, R. C.; Cohen, R. E. *Rheol. Acta* **1981**, *20*, 163–178.
(65) Stadler, F. J.; Münstedt, H. *J. Non-Newtonian Fluid Mech.* **2008**, *151*, 129–135.
(66) Stadler, F. J.; Münstedt, H. *J. Non-Newtonian Fluid Mech.* **2008**, *151*, 227.
(67) Raju, V. R.; Rachapudy, H.; Graessley, W. W. *J. Polym. Sci., Part B: Polym. Phys.* **1979**, *17* (7), 1223–1235.
(68) Carella, J. M.; Graessley, W. W.; Fetters, L. J. *Macromolecules* **1984**, *17* (12), 2775–2786.
(69) Stadler, F. J., *Molecular Structure and Rheological Properties of Linear and Long-Chain Branched Ethene-/α-Olefin Copolymers*; Sierke-Verlag: Göttingen, Germany, 2007.
(70) This conclusion can only be drawn due to the similarity of the effect with respect to the rheological behavior of the *long-chain branches* and of a high molecular tail in the linear sample.
(71) Yang, Q.; Jensen, M. D.; McDaniel, M. P. *Macromolecules* **2010**.
(72) Stadler, F. J.; Becker, F.; Kaschta, J.; Buback, M.; Münstedt, H. *Rheol. Acta* **2009**, *48* (5), 479–490.
(73) Beigzadeh, D.; Soares, J. B. P.; Hamielec, A. E. *J. Appl. Polym. Sci.* **1999**, *71*, 1753–1770.
(74) Kraus, G.; Gruver, J. T. *J. Polym. Sci., Part A: Gen. Pap.* **1965**, *3* (1), 105–122.
(75) Toporowski, P. M.; Roovers, J. *Polymer* **1986**, *24*, 3009–3019.
(76) Hadjichristidis, N.; Roovers, J. *Polymer* **1985**, *26*, 1087–1090.
(77) Roovers, J.; Hadjichristides, N.; Fetters, L. J. *Macromolecules* **1983**, *16*, 214–220.
(78) Graessley, W. W.; Roovers, J. *Macromolecules* **1979**, *12* (5), 959–965.
(79) Roovers, J.; Toporowski, P. M. *J. Polym. Sci., Polym. Phys. Ed.* **1980**, *18* (9), 1907–17.
(80) Fetters, L. J.; Kiss, A. D.; Pearson, D. S.; Quack, G. F.; Vitus, F. J. *Macromolecules* **1993**, *26* (4), 647–654.
(81) Pearson, D. S.; Helfand, E. *J. Polym. Sci., Part B: Polym. Phys.* **1983**, *21*, 2287–2298.
(82) Pearson, D. S.; Helfand, E. *Macromolecules* **1984**, *17* (4), 888–895.
(83) McLeish, T. C. B.; Allgaier, J.; Bick, D. K.; Bishko, G.; Biswas, P.; Blackwell, R.; Blottière, B.; Clarke, N.; Gibbs, B.; Groves, D. J.; Hakiki, A.; Heenan, R. K.; Johnson, J. M.; Kant, R.; Read, D. J.; Young, R. N. *Macromolecules* **1999**, *32* (20), 6734–6758.
(84) Ball, R. C.; McLeish, T. C. B. *Macromolecules* **1989**, *22*, 1911–1913.
(85) Doi, M.; Edwards, S. F., *The Theory of Polymer Dynamics.*; Oxford Press: Oxford, U.K., 1986.
(86) Archer, L. A.; Varshney, S. K. *Macromolecules* **1998**, *31* (18), 6348–6355.
(87) Matsumiya, Y.; Watanabe, H.; Sato, T.; Osaki, K. *Nihon Reoroji Gakkaishi* **1999**, *27* (2), 127–128.
(88) Hadjichristidis, N.; Xenidou, M.; Iatrou, H.; Pitsikalis, M.; Poulos, Y.; Avgeropoulos, A.; Sioula, S.; Paraskeva, S.; Velis, G.; Lohse, D. J.; Schulz, D. N.; Fetters, L. J.; Wright, P. J.; Mendelson, R. A.; Garcia-Franco, C. A.; Sun, T.; Ruff, C. J. *Macromolecules* **2000**, *33* (7), 2424–2436.
(89) Knauss, D. M.; Huang, T. Z. *Macromolecules* **2002**, *35* (6), 2055–2062.
(90) Heinrich, M.; Pyckhout-Hintzen, W.; Allgaier, J.; Richter, D.; Straube, E.; Read, D. J.; McLeish, T. C. B.; Groves, D. J.; Blackwell, R. J.; Wiedenmann, A. *Macromolecules* **2002**, *35* (17), 6650–6664.
(91) Young, R. N.; Hakiki, A.; McLeish, T. C. B. *Book of Abstracts*, 212th ACS National Meeting, Orlando, FL, August 25−29 1996, POLY-307.

(92) Roovers, J. *Polym. Prepr. (Am. Chem. Soc., Div. Polym. Chem.)* **1979**, *20* (2), 144–148.
(93) Roovers, J.; Graessley, W. W. *Macromolecules* **1981**, *14* (3), 766–773.
(94) Roovers, J. *Macromolecules* **1984**, *17* (6), 1196–200.
(95) McLeish, T., C, B. *Macromolecules* **1988**, *21*, 1062–1070.
(96) Hakiki, A.; Young, R. N.; McLeish, T. C. B. *Macromolecules* **1996**, *29* (10), 3639–41.
(97) Daniels, D. R.; McLeish, T. C. B.; Crosby, B. J.; Young, R. N.; Fernyhough, C. M. *Macromolecules* **2001**, *34* (20), 7025–7033.
(98) Inkson, N. J.; Graham, R. S.; McLeish, T., C, B.; Groves, D. J.; Fernyhough, C. M. *Macromolecules* **2006**, *39* (12), 4217–4227.
(99) According to Park et al.,[100] long-chain branched chains can also reptate, but only after *all* side chains have relaxed by fluctuation.
(100) Park, S. J.; Shanbhag, S.; Larson, R. G. *Rheol. Acta* **2005**, *44* (3), 319–330.
(101) McLeish, T. C. B. *Adv. Phys.* **2002**, *51* (6), 1379–1527.
(102) Dealy, J.; Larson, R. G., *Structure and Rheology of Molten Polymers - From Structure to Flow Behavior and Back Again*. Hanser: Munich, Germany, 2006.
(103) Although using a double logarithmic mixing rule does not have a theoretical foundation, it often leads to good results.
(104) Stadler, F. J.; Mahmoudi, T. *J. Rheol.* **2011**, Submitted for publication.